Title: The homeodomain transcription factor Hb9 controls axon guidance in *Drosophila* through the regulation of Robo receptors

Authors: Celine Santiago, Juan-Pablo Labrador and Greg J. Bashaw

Supplemental Information

Supplemental Data

Supplemental Experimental Procedures

Supplemental References

Figure S1, Related to Figure 1

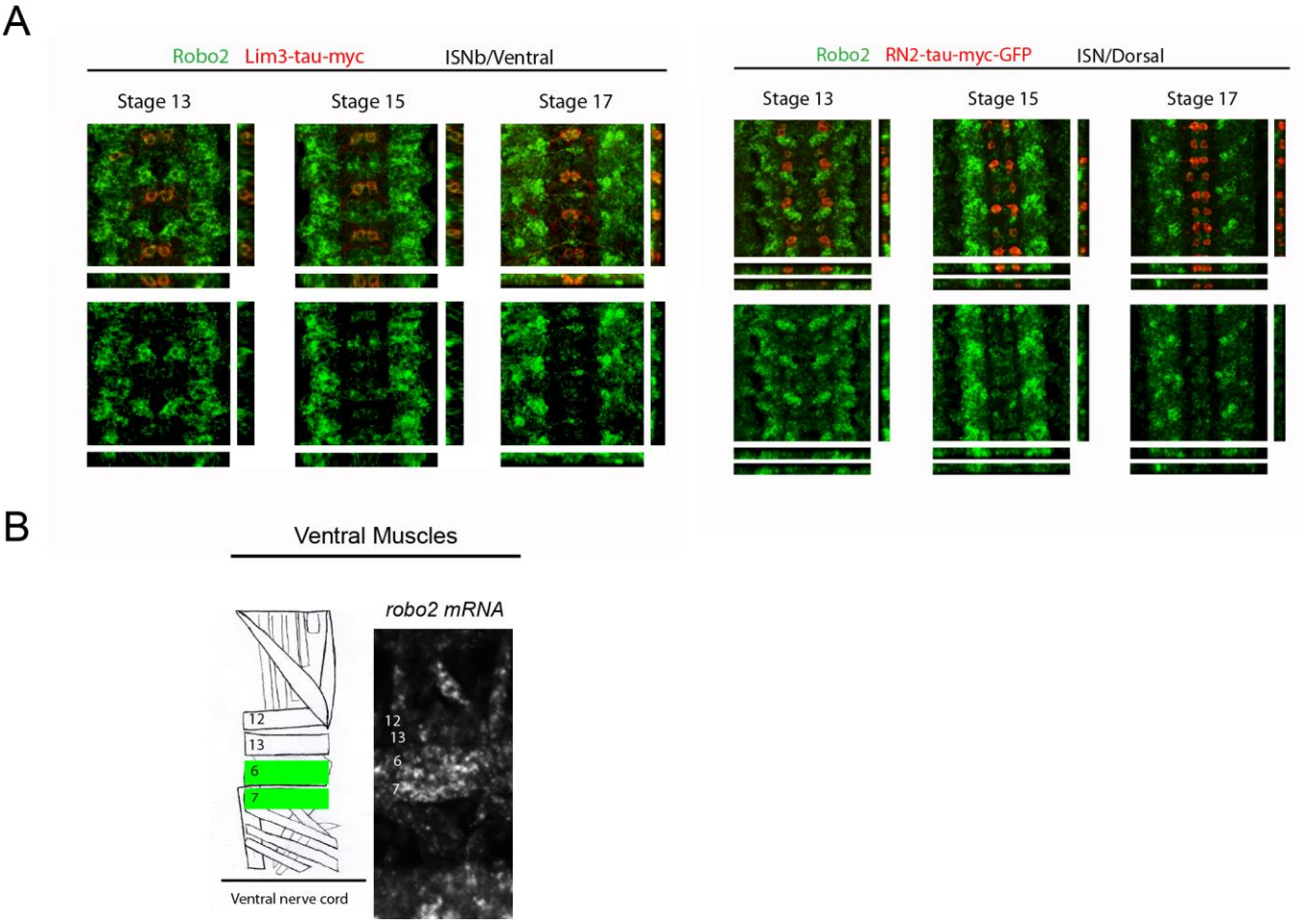

Figure S1, Related to Figure 1: *Robo2* mRNA is enriched in ventrally projecting motor neurons and their muscle targets. A: Fluorescent *in situ* for *robo2* mRNA (green). Anterior is up. A, Left: *Robo2* mRNA is detected in the ventrally-projecting RP motor neurons, labeled by the *lim3a-tau-myc* transgene (red), at Stages 13-15, as the RP motor axons explore the ventral muscle field, and persists into Stage 17, when the axons form their final arborizations. A, Right: *Robo2* mRNA is detected in the dorsally-projecting motor neurons aCC and RP2, labeled by *RN2Gal4>UAS-TauMycGFP* (red) during the early stages of motor axon pathfinding (Stage 13). During Stages 15-17, when the ISN targets dorsal muscle regions, *robo2* is no longer enriched in aCC/RP2. B: Stage 16 embryo, dorsal is up. *Robo2* is expressed in the ventral muscles 7 and 6, which are labeled in green in the cartoon.

Figure S2, Related to Figure 2

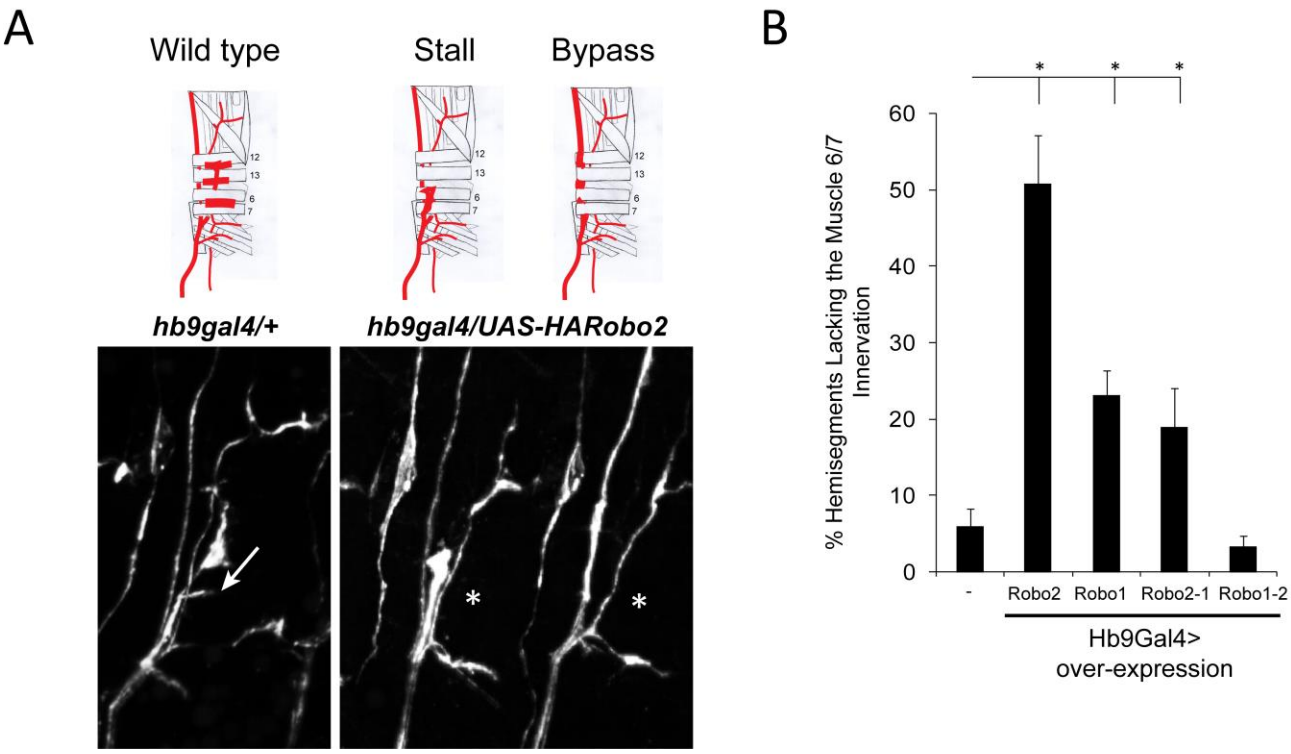

Figure S2, Related to Figure 2: Robo2 gain of function in motor neurons causes motor axon innervation defects; Robo2-1 (Ecto-Cyto) gain of function also causes defects whereas Robo1-2 does not. A: Stage 17 embryos stained for Fasciclin II to label all motor axons. Anterior is left. The arrow points to the muscle 6/7 innervation, while asterisks indicate its absence. *Robo2* over-expression using *hb9gal4* causes 6/7 innervation defects due to stalling and bypass phenotypes. B: The percentage of hemisegments lacking the muscle 6/7 innervation was quantified in late Stage 17 embryos. Asterisks indicate a significant difference ($p<0.05$) compared to controls. Error bars = s.e.m. *Robo2 over-expression* denotes [*UAS-HARobo2]86FB/hb9gal4. Robo1 over-expression* denotes [*UAS-HARobo1]86FB/hb9gal4. Robo2-1 over-expression* denotes [*UAS-HARobo2-1].T6/hb9gal4. Robo1-2 over-expression* denotes *[UAS-HARobo1-2].T39/+; hb9gal4/+*.

Figure S3, Related to Figure 4

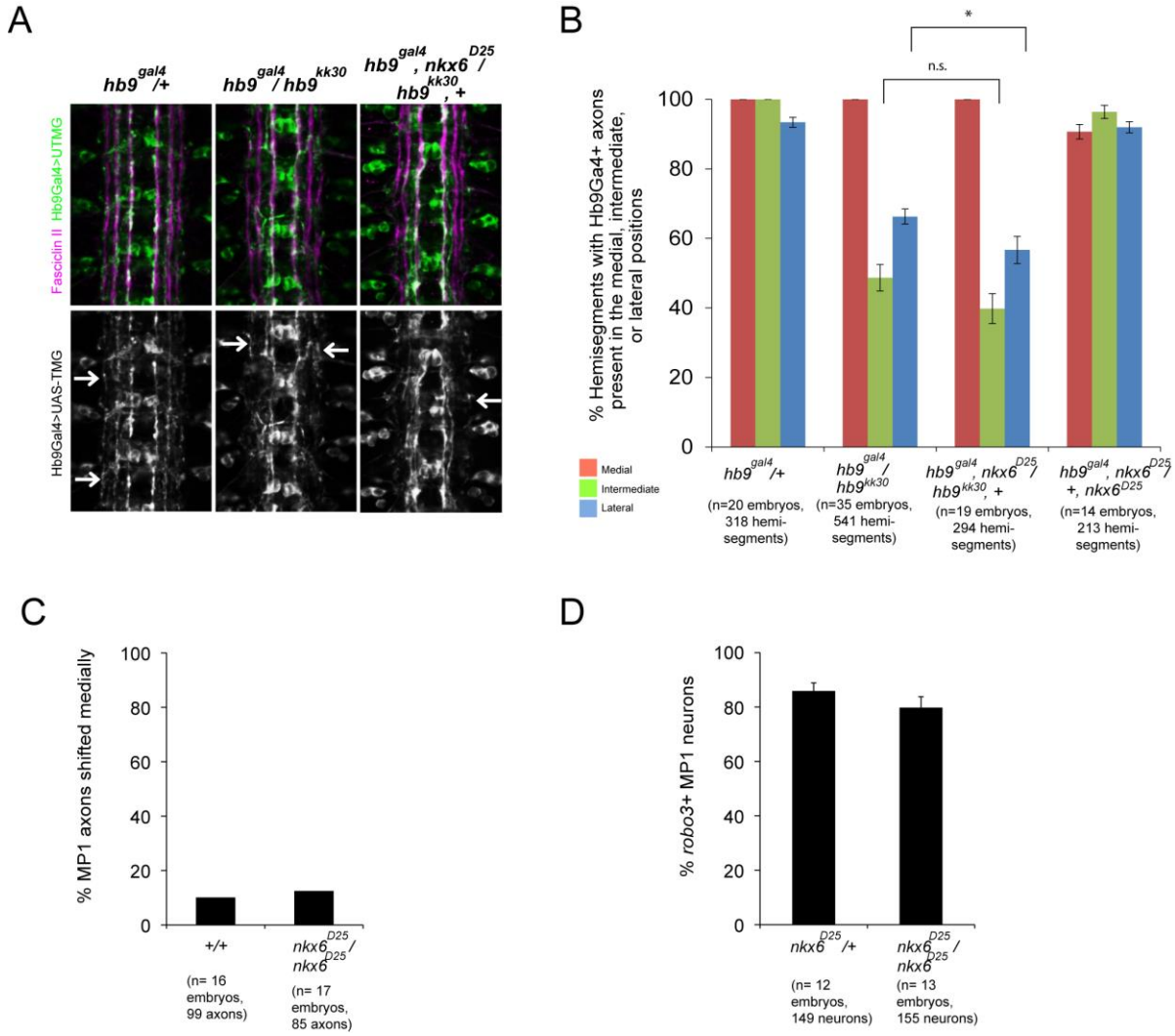

Figure S3, Related to Figure 4: *Nkx6* is not required for the lateral pathway selection of *hb9gal4*+ axons or for *robo3* expression in MP1 neurons, but loss of *nkx6* dominantly enhances the lateral pathway defects of *hb9* mutants. A: Stage 17 embryos, anterior is up. *Hb9gal4>UAS-TauMycGFP* labels three longitudinal pathways (green) which align with FasII+ pathways (magenta). Arrows point to the lateral-most *hb9gal4* pathway, which is often disrupted in *hb9* mutants and *hb9* mutants heterozygous for *nkx6*. B: Quantification of *hb9gal4*+ axons in the medial, intermediate, or lateral positions. Loss of *nkx6* dominantly enhances the lateral pathway defects of *hb9* mutants (Student's t-test, p = 0.026) but causes no significant change in

the intermediate pathway. *Nkx6* mutants heterozygous for *hb9* have no significant defects in *hb9gal4+* lateral pathways. C, D: *Nkx6* mutants have no defects in the lateral position of the MP1 axon, or in *robo3* expression in MP1. Error bars = s.e.m.

Figure S4, Related to Figure 5

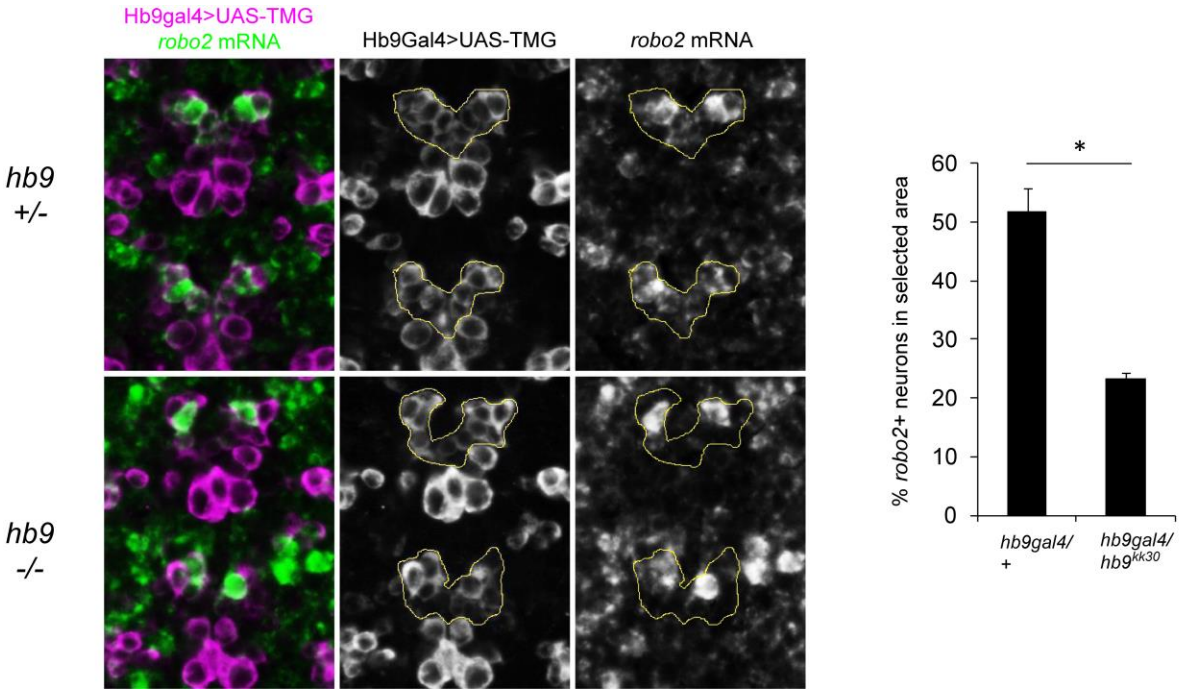

Figure S4, Related to Figure 5: *Hb9* is required for *robo2* expression in a subset of CNS neurons. A: Fluorescent *in situ* hybridization for *robo2* mRNA (green) in Stage 15 embryos; anterior is up. *Hb9gal4>UAS-TauMycGFP* (magenta) labels a V-shaped cluster of neurons, outlined in yellow in the single-channel images. In *hb9* heterozygotes, most of these cells are positive for *robo2* mRNA, whereas there are fewer *robo2+* neurons in this cluster in *hb9* mutants. B: The percentage of *robo2+/hb9gal4+* neurons in the region of interest was quantified for *hb9* heterozygous and mutant embryos. *Hb9* mutants have a significant decrease compared to heterozygous siblings ($p<0.0001$, Student's t-test). Error bars = s.e.m.

Figure S5, Related to Figure 7

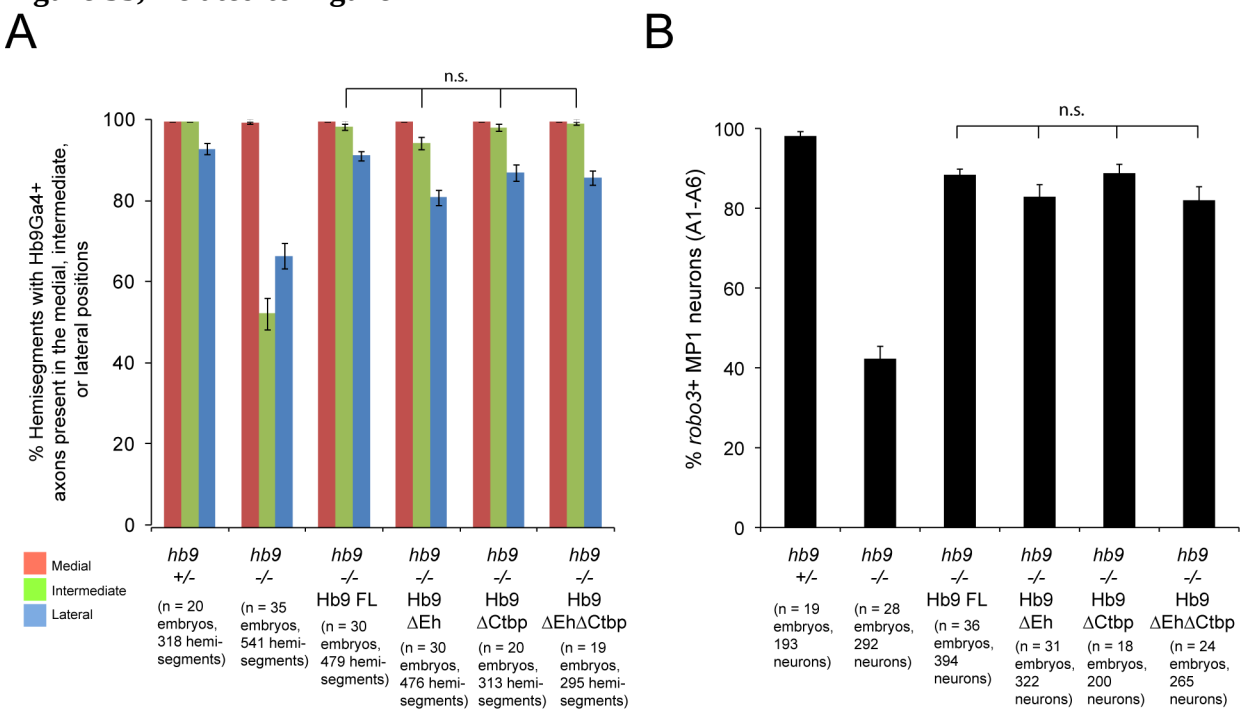

Figure S5, Related to Figure 7: Neither of Hb9's putative repressor domains is required for rescuing the lateral position defects of *hb9gal4+* intermediate axons, or for *robo3* expression in MP1 neurons. A: The presence of *hb9gal4+* axons in the medial, intermediate, or lateral positions is shown for each genotype. Over-expression of a full-length Hb9 transgene fully rescues the defects in the intermediate *hb9gal4+* pathway (green bar), as does over-expression of Hb9ΔEh, Hb9ΔCtBP, and Hb9ΔEhΔCtBP. B: The percentage of MP1 neurons expressing *robo3* mRNA was quantified for each genotype. Over-expression of Hb9 in *hb9* mutants rescues *robo3* expression, as does over-expression of Hb9ΔEh, Hb9ΔCtBP, and Hb9ΔEhΔCtBP. Error bars = s.e.m. In panel A, *hb9 +/-* denotes $hb9^{gal4}/TM3$. In panel B, *hb9 +/-* denotes $hb9^{ad121}/TM3$. In panels A and B, *hb9 -/-* denotes $hb9^{gal4}/hb9^{kk30}$ and *hb9 -/- Hb9 (variant)* denotes *UAS-Hb9 (variant)/+;* $hb9^{gal4}/hb9^{kk30}$.

Supplemental Experimental Procedures

Genetics

The following alleles were used: *robo2*^{x123} (Simpson et al., 2000a); *robo2*^{x33} (Simpson et al., 2000a); *hb9*^{kk30}, *hb9*^{ad121}, *hb9*^{JJ154e}, *hb9*^{gal4} (Broihier et al., 2002); *nkx6*^{D25} (Broihier et al., 2004); *ap*^{Gal4} (O'Keefe et al., 1998); *robo3*^{1} (Rajagopalan 2000b); *robo3*^{3} (Pappu et al., 2011); *Df(2L)ED108* (Ryder et al., 2007); *robo2*^{robo2}, *robo2*^{robo1}, *robo2*^{robo3}, *robo2*$^{robo2-1}$, *robo2*$^{robo1-2}$ (Spitzweck et al., 2010); *robo2*^{F} (gift from L. Zipursky). *Robo2*^{F} is a loss of function allele generated by EMS mutagenesis on the *robo3*^{3} chromosome. The following transgenes were used: *UAS-Robo2RNAi* (Vienna *Drosophila* Research Center); *C544-Gal4* (Wheeler et al., 2006); *UAS-Hb9* (Broihier et al., 2002); *isletH-tau-myc* (Thor et al., 1997); *lim3A-tau-myc* (Thor et al., 1999); *lim3b-gal4* (Certel et al., 2004); *[UAS-HARobo1-2].T*39, *[UAS-HARobo2-1].T6, [UAS-HARobo2].T1, [UAS-HARobo3].T15* (Evans et al., 2010); *[UAS-HARobo2]86FB, [UAS-HARobo1]86FB* (Evans et al., 2012); *UAS-Tau-Myc-GFP*, *ftz-ngGal4*, *24b-gal4*, *RN2-Gal4* (Bloomington Stock Center); *[UAS-Hb9 FL]51C, [UAS-Hb9 ΔEh]51C, [UAS-Hb9 ΔCtBP]51C, [UAS-Hb9 ΔEhΔCtBP]51C*, [*22K18-robo2BAC]51C*. All crosses were performed at 25°C. Embryos were genotyped using a combination of marked balancer chromosomes or the presence of tagged transgenes.

Immunostaining

Embryo fixation and staining were performed as described (Kidd et al., 1998). The following antibodies were used: mouse MAb 1D4/Fasciclin II [Developmental Studies Hybridoma Bank (DSHB); 1:100], mouse anti-ßgal (DSHB; 1:150), mouse anti-HA (Covance #MMS-101P; 1:250), rabbit anti-GFP (Invitrogen #A11122; 1:500), rabbit anti-c-Myc (Sigma #C3956; 1:500), chick anti- ßgal (Abcam #9361; 1:1000), guinea pig anti-Hb9 (gift from J. Skeath; 1:1000), Cy3

goat anti-mouse (Jackson #115-165-003; 1:1000), Alexa-488 goat anti-rabbit (Molecular Probes #A11008; 1:500), Cy3 goat anti-chick (Abcam #97145; 1:500), Alexa-647 goat anti-Guinea Pig (Molecular Probes #A-21450; 1:500).

Fluorescent *in situ* quantification

Fluorescent *in situ* hybridization was performed as described (Labrador et al., 2005). Max projections were obtained for embryos from the same collection. A region of interest (ROI) was generated around the RP cell bodies in ImageJ software, using the *islet-tau-myc* staining as a reference. Total fluorescence intensity above a set threshold was obtained for each channel by multiplying the area of the ROI by the average fluorescence intensity within the ROI above the threshold. Relative fluorescence intensity of *robo2* mRNA was calculated as absolute *robo2* mRNA fluorescence intensity divided by absolute myc fluorescence intensity.

Phenotypic quantification

Phenotypes were scored using Volocity imaging software. For scoring *robo2* and *robo3* expression, if the cell body of a neuron could be detected by the *in situ* signal, that neuron was scored as positive. RP3 neurons were identified by using *islet-tau-myc* and their position; ventral apterous neurons were identified by using *apGal4* and their position; MP1 neurons were identified by using *C544-Gal4*, FasII, and their position. For motor axon phenotypes, hemisegments in which a FasII+ axon could not be detected between the cleft of ventral muscles 6 and 7 were scored as lacking the muscle 6/7 innervation. A2-A6 were scored in late Stage 17 embryos. For *Hb9Gal4+* axon phenotypes, the presence of the medial, intermediate, or lateral *hb9gal4+* axon bundles was scored for hemisegments in A1-A8 in Stage 17 embryos. If a bundle

could not be detected or was visibly shifted to another lateral zone, it was scored as absent. For apterous lateral shift phenotypes, if a hemisegment contained an apterous axon that projected along the intermediate or lateral FasII tracts, it was scored as shifted. A1-A8 were scored in Stage 17 embryos. For MP1 axon phenotypes, the lateral position of MP1 axons was scored relative to the FasII pathways. A1-A7 were scored in Stage 16-17 embryos. For statistical analysis, comparisons were made between genotypes using the Student's t-test or Fisher's exact test, as indicated in the figure legends. Embryos were scored blind to genotype when possible.

Supplemental References

Evans TA, Bashaw GJ. (2012). Slit/Robo-mediated axon guidance in Tribolium and Drosophila: divergent genetic programs build insect nervous systems. Dev Biol. 363(1):266-78.

O'Keefe DD, Thor S, Thomas JB. (1998). Function and specificity of LIM domains in Drosophila nervous system and wing development. Development. 25(19): 3915-23.

Pappu KS, Morey M, Nern A, Spitzweck B, Dickson BJ, Zipursky SL. (2011). Robo-3-mediated repulsive interactions guide R8 axons during Drosophila visual system development. Proc Natl Acad Sci U S A. 108(18):7571-6.

Ryder E, Ashburner M, Bautista-Llacer R, Drummond J, Webster J, Johnson G, Morley T, Chan YS, Blows F, Coulson D, Reuter G, Baisch H, Apelt C, Kauk A,Rudolph T, Kube M, Klimm M, Nickel C, Szidonya J, Maróy P, Pal M, Rasmuson-Lestander A, Ekström K, Stocker H, Hugentobler C, Hafen E, Gubb D, Pflugfelder G, Dorner C, Mechler B, Schenkel H, Marhold J, Serras F, Corominas M, Punset A, Roote J, Russell S. (2007). The DrosDel deletion collection: a Drosophila genomewide chromosomal deficiency resource. Genetics. 177(1):615-29.